Inorg. Chem. **2008**, *47*, 306–314

Inorganic Chemistry

Article

Heterometallic Cuboidal Clusters $M_3M'Q_4$ (M = Mo, W; M′ = Sn, Pb, As, Sb; Q = S, Se): From Coordination Compounds to Supramolecular Adducts

Rita Hernández-Molina,*,[†] Irina V. Kalinina,[‡] Pavel A. Abramov,[‡] Maxim N. Sokolov,[‡] Alexandr V. Virovets,[‡] Javier G. Platas,[§] Rosa Llusar,[§] Victor Polo,[§] Cristian Vicent,[§] and Vladimir P. Fedin[‡]

Departamento de Química Inorgánica, Universidad de La Laguna, 38200 La Laguna, Tenerife, Islas Canarias, Spain, Nikolaev Institute of Inorganic Chemistry, Prospect Lavrentyeva 3, 630090 Novosibirsk, Russia, and Departament de Química Física i Analítica, Universitat Jaume I, Avda. Sos Baynat s/n, E-12071 Castelló, Spain

Received August 8, 2007

Reactions of the incomplete cuboidal clusters $[M_3Q_4(acac)_3(py)_3]^+$ (M = Mo, W; Q = S, Se) with group 14 and 15 metal complexes with the s^2p^0 electronic configuration ($AsPh_3$, $SbPh_3$, $SbCl_3$, SbI_3, PbI_3^-, $SnCl_3^-$) led to heterometal incorporation with the formation of cuboidal clusters of the type $[M_3(EX_3)Q_4(acac)_3(py)_3]^{n+}$ ($n = 0$ for Sn, Pb; $n = 1$ for As, Sb), whose structures were determined by X-ray diffraction. The cuboidal clusters can be described as complexes of the cluster tridentate ligand $[M_3Q_4(acac)_3(py)_3]^+$ (μ_2-chalcogen atoms as donors) with the EX_3, where the E atom attains a distorted octahedral coordination. Analysis based on the bond distances E–Q gives the following sequence of affinity: As < Sb; Pb < Sn ≈ Sb; $SbPh_3 < SbI_3 \approx SbCl_3$; $W_3S_4 < W_3Se_4$. Interaction energies at the gas phase between $[W_3Q_4(acac)_3(py)_3]^+$ (Q = S, Se) and SbX_3 (X = I, Ph) were computed at the DFT level (BP86/TZP). The magnitude of the interaction depends strongly on the substituents at Sb, and the replacement of iodine by the phenyl group decreases the interaction energy from –9.21 to –2.70 kcal/mol and from –12.73 to –3.85 kcal/mol for the W_3SbS_4 and W_3SbSe_4 cores, respectively.

Introduction

Triangular chalcogenide-bridged clusters of Mo and W, $M_3(\mu_3\text{-}Q)(\mu_2\text{-}Q)_3^{4+}$ (Q = S, Se), have a unique ability to incorporate post-transition metals of 12−15 groups in low and intermediate oxidation states (electronic configurations s^2), to form cuboidal clusters of the $M_3M'(\mu_3\text{-}Q)_4^{(4+n)+}$ type,[1] first reported by Lu in 1987[2] (M′ = Ga, In, $n = 1$; Ge, Sn, Pb, $n = 2$; As, Sb, Bi, $n = 3$). Other examples followed suit.[3] Though this incorporation does not lead to bonding between M and M′ (M···M′ distances are quite long, 3.8−4.0 Å), it stabilizes the M_3 cluster framework, as evidenced from shortening of the M−M bonds. At least in the case of Sn(II), calculations and physical measurements indicate a charge transfer from Sn to M (Mo or W), which can be, perhaps oversimplistically, described in terms of Sn(II) → Sn(IV) oxidation.[3b] The situation is less clear-cut for other metals because, for example, Pb(II) or Sb(III) are not easy oxidized. Most of the synthetic work was done on the sulfide clusters, and very little is known about their selenide analogues. An additional point of interest is added by possible applications due to interesting nonlinear optic properties of some of these compounds.[4] In this work, we report reactions of the incomplete cuboidal clusters $[M_3Q_4(acac)_3(py)_3]^+$ (M = Mo, W; Q = S, Se) and their dmpe and NCS derivatives with group 14 and 15 metal compounds having an s^2p^0 electronic configuration and substituents of different electronegativity at the metal ($AsPh_3$, $SbPh_3$, $SbCl_3$, SbI_3, PbI_3^-, $SnCl_3^-$), together with their structural characterization and quantum chemical studies.

---

* To whom correspondence should be addressed. E-mail: caesar@che.nsk.su.

[†] Universidad de La Laguna.

[‡] Nikolaev Institute of Inorganic Chemistry.

[§] Universitat Jaume I.

(1) Hernandez-Molina, R.; Sokolov, M. N.; Sykes, A. G. *Acc. Chem. Res.* **2001**, *34*, 223.

(2) (a) Lu, S.-F.; Huang, J.-Q.; Lin, Y.-H.; Huang, J.-L. *Acta Chim. Sinica* **1987**, *3*, 191. (b) Yu, R.-M. (b) Lu, S.-F.; Huang, J.-Q.; Huang, X.-Y.; Wu, Q.-J.; Wu, D.-X. *Inorg. Chem.* **2000**, *39*, 5348.

10.1021/ic701581u CCC: $40.75

Experimental Section

All of the manipulations were done in air. The starting triangular complexes $[M_3Q_4(acac)_3(py)_3]PF_6$ (Q = S, Se) $[Mo_3S_4(dmpe)_3Cl_3]PF_6$ and $(Et_4N)_5[W_3S_4(NCS)_9]$ were prepared according to the published procedures.$^{5-7}$ The solvents were reagent quality and used as purchased. $SbCl_3$, SbI_3, $SbPh_3$, $AsPh_3$, and $SnCl_2$ were from Aldrich and used without further purification. $KPbI_3$ was prepared according to ref 3l. Electronic spectra were recorded on a Shimazu UV-2101PC spectrometer. Elemental analysis was performed on an EA 1108 CHNS−O micro analytical analyzer. A Quattro LC (quadrupole-hexapole-quadrupole) mass spectrometer with an orthogonal Z-spray electrospray interface (Micromass, Manchester, UK) was used.

$[Mo_3(AsPh_3)S_4(acac)_3(py)_3]PF_6\cdot 3MeCN$ (1-AsPh). To a solution of $[Mo_3S_4(acac)_3(py)_3]PF_6$ in CH_3CN (0.5 g, 0.48 mmol) $AsPh_3$ (0.15 g, 0.48 mmol) was added. A dark-green solution was left in an open vial for 4 days, and green crystalline solid formed. It was filtered, washed with ether, and dried in air. Yield 35% (0.25 g). Anal. Calcd for $Mo_3AsC_{54}H_{60}S_4O_6N_6PF_6$: C, 42.5; N, 5.5; H, 4.0. Found: C, 42.1; N, 5.8; H, 3.9. IR (cm^{-1}, KBr): 3051(w), 2924(w), 2855(w), 1571(vs), 1527(s), 1484(m), 1444(s), 1366(s), 1280(s), 1220(s), 1187(w), 1157(w), 1123(w), 1070(s), 1025(s), 964(w), 936(w), 841(vs) (PF_6),740(s), 695(s), 668(w), 636(w), 557(s), 487(m), 475(m), 433(s).

$[Mo_3S_4Cl_3(dmpe)_3]SnCl_3$ (1′-SnCl). To a colorless solution of $SnCl_2\cdot 2H_2O$ (0.016 g, 0.07 mmol) and Bu_4NCl (0.010 g, 0.018 mmol) in EtOH was added a dichloromethane solution of $[Mo_3S_4Cl_3(dmpe)_3]PF_6$ (0.04 g, 0.036 mmol) in CH_2Cl_2 (20 mL). The reaction was stirred for 15 min, and the color of the solution turns brown immediately. The resulting solution was taken to dryness, washed thoroughly with water, EtOH (3 × 2 mL), and ether. Yield 65% (0.028 g). Suitable single crystals were obtained by slow evaporation of solutions in CH_2Cl_2. UV−vis in CH_2Cl_2, λ(nm): 331, 405, 469 (sh); in CH_3CN, λ(nm): 341, 398. ESI-MS (CH_2Cl_2, 15 V) m/z: 973 $[Mo_3S_4Cl_3(dmpe)_3]^+$

$[Mo_3(SnCl_3)Se_4(acac)_3(CH_3CN)_3]\cdot 2H_2O$ (2-SnCl). To a solution of $[Mo_3Se_4(acac)_3(py)_3]PF_6$ in CH_3CN (0.5 g, 0.39 mmol) an equimolar amount of anhydrous $SnCl_2$ (0.15 g, 0.80 mmol) was added. A dark-brown solution was left in an open vial for 7 days, and a dark-brown crystalline solid formed. It was filtered, washed with ether, and dried in air. Yield 40% (0.20 g).

$[W_3(SbI_3)S_4(acac)_3(py)_3]I_5$ (3-SbI). Red-brown crystals of this compound were obtained from $[W_3S_4(acac)_3(py)_3]PF_6$ (0.5 g, 0.39 mmol) in CH_3CN and SbI_3 (0.8 g, 1.60 mmol) in CH_3CN after mixing and allowing the solvent to evaporate slowly. Yield 30% (0.27 g). IR (cm^{-1}, KBr): 3438(w), 3000(w), 2319(w), 2135(w), 1604(w), 1563(vs), 1531(vs), 1492(w), 1444(s), 1421(m), 1359(s), 1286(s), 1221(m), 1192(w), 1158(w), 1068(m), 1026(s), 938(m), 842(vs), 759(m), 695(s), 671(s), 558(s), 467(w), 444(m), 419(w).

$[W_3(SbPh_3)S_4(acac)_3(py)_3]PF_6$ (3-SbPh). Similarly, red-brown crystals of this compound were obtained from $[W_3S_4(acac)_3(py)_3]PF_6$ (0.5 g, 0.39 mmol) and $SbPh_3$ (0.14 g, 0.4 mmol) in CH_3CN. Yield 35% (0.23 g). Anal. Calcd for $W_3SbC_{48}H_{51}S_4O_6N_3PF_6$: C, 33.7; N, 2.5; H, 3.0. Found: C, 34.3; N, 2.3; H, 3.3. IR (cm^{-1}, KBr): 3437(w), 3046(w), 1965(w), 1606(m), 1575(vs), 1531(vs), 1487(w), 1448(s), 1429(s), 1370(s), 1358(m), 1283(s), 1222(s), 1189(m), 1158(m), 1069(s), 1044(m), 1018(s), 998(w), 937(m), 874(w), 841(v)s, 783(w), 769(w), 762(w), 737(s), 695(s), 670(m), 652(w), 637(w), 557(vs), 466(m), 456(w), 439(m), 422(w).

$[W_3(SnCl_3)S_4(acac)_3(py)_3]$ (3-SnCl). Red-brown crystals of this compound were obtained from $[W_3S_4(acac)_3(py)_3]PF_6$ (0.5 g, 0.39 mmol) in CH_3CN and $SnCl_2$ (0.3 g, 0.80 mmol). Yield 40% (0.22 g). Anal. Calcd for $W_3SnCl_3C_{36}O_6N_3S_4$: C, 25.0; N, 2.9; H, 2.5. Found: C, 25.0; N, 2.7; H, 2.9. IR (cm^{-1}, KBr): 3334 (s), 3208(w), 3152(w), 3121(m), 2923(w), 1647(s), 1609(s), 1564(s), 1538(s), 1490(m), 1445(m), 1425(m), 1367(s), 1284(s), 1256(w), 1221(m), 1176(w), 1121(w), 1069(s), 1028(s), 1015(s), 935(m), 840(s), 743(s), 695(w), 674(s), 558(s), 462(w), 439(s). UV−vis (CH_3CN, nm): 216, 255, 300(sh), 404.

$[W_3(PbI_3)S_4(acac)_3(py)_3]\cdot 1.7CH_3CN$ (3-PbI). In a similar way, violet-brown crystals of the compound were obtained from $[W_3S_4(acac)_3(py)_3]PF_6$ (0,5 g, 0.39 mmol) and $KPbI_3$ (0.25 g, 0.40 mmol) in CH_3CN. Yield 40% (0.29 g). Anal. Calcd for $W_3PbI_3C_{30}H_{36}O_6N_3S_4$: C, 20.0; N, 2.3 H, 2.0. Found: C, 18.9; N, 2.4; H, 2.0. IR (cm^{-1}, KBr): 3437(w), 2136(w), 1568(vs), 1530(vs), 1444(m), 1420(w), 1365(s), 1287(s), 1221(m), 1159(w), 1069(m), 1025(s), 938(m), 874(w), 814(vs), 760(m), 696(s), 674(w), 638(w), 559(s), 468(w), 446(m).

$[W_3(SbCl_3)S_4(acac)_3(py)_3]PF_6$ (3-SbCl). To a solution of 50 mg (0.037 mmol) $[W_3S_4(acac)_3(py)_3]PF_6$ in 10 mL of $CHCl_3$ 9 mg (0.039 mmol) of $SbCl_3$ were added. The color of the solution rapidly turned red, and a bright-red microcrystalline solid started to appear. The next day, it was filtered off, washed with ether, and dried. Anal. Calcd for $C_{30}H_{36}N_3Cl_3F_6O_6PSbS_4W_3$: C, 22.6; H 2.3; N, 2.6; S, 8.1. Found: C, 22.6; H 2.2; N 2.7; S, 7.4. IR (cm^{-1}, KBr): 3434(s), 3332(m), 3229(m), 3166(m), 3099(w), 3071(m), 2960(m), 2923(m), 2859(w), 2318(w), 2293(w), 1635(s), 1608(s), 1560(s), 1533(s), 1421(m), 1359(s), 1286(s), 1241(w), 1196(w), 1160(w), 1029(s), 835(s), 741(s), 673(s), 558(s), 483(s), 421(w).

$(pyH)[W_3(SbCl_3)S_4(acac)_3(py)_3][Sb_2OCl_6]\cdot Me_2CO\cdot MeCN$ (3-SbCl′). These bright-red single crystals were obtained by recrystallization of **3-SbCl** from 1:1 (v/v) acetone/acetonitril mixture.

$(Et_4N)_5[W_3(SbI_3)S_4(NCS)_9]$ (3-SbI−NCS). To a solution of $(Et_4N)_5[W_3S_4(NCS)_9]$ (0.30 g, 0.16 mmol) in 10 mL of acetone,

---

(3) (a) Varey, J. E.; Lamprecht, G. J.; Fedin, V. P.; Holder, A.; Clegg, W.; Elsegood, M. R. J.; Sykes, A. G. *Inorg. Chem.* **1996**, *35*, 5525. (b) Müller, A.; Fedin, V. P.; Diemann, E.; Bögge, H.; Krickemeyer, E.; Sölter, D.; Giuliani, A. M.; Barbieri, R.; Adler, P. *Inorg. Chem.* **1994**, *33*, 2243. (c) Keck, H.; Kruse, A.; Kuchen, W.; Mootz, D.; Wiskemann, R.; Wunderlich, H. *Z. Naturforsch.* **1989**, *45b*, 461. (d) Fedin, V.P.; Sokolov, M.N.; Sykes, A.G. *J. Chem. Soc., Dalton Trans.* **1996**, 4089. (e) Hernández-Molina, R.; Fedin, V.; Sokolov, M. N.; Saysell, D.; Sykes, A. G. *Inorg. Chem.* **1998**, *37*, 4328. (f) Hernández-Molina, R.; Dybtsev, D. N.; Fedin, V. P.; Elsegood, M. R. J.; Clegg, W.; Sykes, A. G. *Inorg. Chem.* **1998**, *37*, 2995. (g) Fedin, V. P.; Sokolov, M. N.; Virovets, A. V.; Podberezskaya, N. V. *Inorg. Chim. Acta* **1998**, *269*, 292. (h) Huang, J. Q.; Lu, S. F.; Huang, X. Y.; Wu, Q. J.; Yu, R. M. *J. Cluster Sci.* **1997**, *8*, 47. (i) Lu, S. F.; Huang, J. Q.; Huang, X. Y.; Wu, Q. J.; Yu, R. M. *Inorg. Chem.* **1999**, *38*, 3801. (j) Lu, S. F.; Huang, J. Q.; Wu, Q. J.; Huang, X. Y.; Wu, D. X.; Zheng, Y.; Yu, R. M. *Polyhedron* **1998**, *18*, 281. (k) Yu, R. M.; Lu, S. F.; Huang, X. Y.; Wu, Q. J.; Huang, J. Q. *Inorg. Chem.* **1999**, *38*, 3313. (l) Lu, S.-F.; Huang, J.-Q., Wu, Q.-X.; Huang, X.-Y.; Yu, R.-M.; Zheng, Y.; Wu, D.-X. *Inorg. Chim. Acta* **1997**, *261*, 201. (m) Sokolov, M.N.; Dybtsev, D.N.; Virovets, A.V.; Clegg, W.; Fedin, V.P. *Izv. Akad. Nauk, Ser. Khim.* **2001**, 1144. (n) Gerasko, O.A.; Virovets, A.V.; Sokolov, M.N.; Dybtsev, D.N.; Gerasimenko, A.V.; Fenske, D.; Fedin, V.P. *Izv. Akad. Nauk, Ser. Khim.* **2002**, 1654. (o) Sokolov, M.N.; Gerasko, O.A.; Dybtsev, D.N.; Chubarova, E.V.; Virovets, A.V.; Vicent, C.; Llusar, R.; Fenske, D.; Fedin, V.P. *Eur. J. Inorg. Chem.* **2004**, 63.

(4) Lu, S.-F.; Huang, J.-Q.; Yu, R.-M.; Huang, X.-Y.; Wu, Q.-J.; Peng, Y.; Chen, J.; Huang, Z.-X.; Zheng, Y.; Wu, D.-X. *Polyhedron*, **2001**, *20*, 2339.

(5) Hernández-Molina, R.; Sokolov, M.; Clegg, W.; Esparza, P.; Mederos, A. *Inorg. Chim. Acta* **2002**, *331*, 52.

(6) Estevan, F.; Feliz, M.; Llusar, R.; Mata, J. A.; Uriel, S. *Polyhedron*, **2001**, *20*, 527.

(7) Fedin, V. P.; Sokolov, M. N.; Gerasko, O. A.; Kolesov, B. A.; Fedorov, V. E.; Mironov, A. V.; Yufit, D. S.; Slovohotov, Yu.L.; Struchkov, Yu.T. *Inorg. Chim. Acta* **1990**, *175*, 217.

0.09 g of SbI_3 (0.18 mmol) was added upon stirring. The stirring continued for 1 h, and after that the vial with the red solution was placed in a jar filled with diethyl ether for 5 days. Dark-red crystalline solid (0.07 g) was collected. Yield 20%. Anal. Calcd for $C_{49}H_{100}N_{14}I_3SbS_4W_3$: C, 25.0; H 4.3; N, 8,3; S, 17.7. Found: C, 24.6; H 4.2; N 8.7; S, 17.5.

$(Et_4N)_5[W_3(BiI_3)S_4(NCS)_9]$ (3-BiI−NCS). To a solution of $(Et_4N)_5[W_3S_4(NCS)_9]$ (0.30 g, 0.16 mmol) in 10 mL of acetonitrile 0.16 g of BiI_3 (0.27 mmol) was added upon stirring. The stirring continued for 1 h, after that 10 mL of diethyl ether was added to the solution, and the flask was stoppered and left at +4 °C overnight. Shiny black crystalline solid (0.15 g) was collected. Yield 38%. Anal. Calcd for $C_{49}H_{100}N_{14}I_3BiS_4W_3$: C, 24.1; H 4.1; N, 8,0; S, 17.0. Found: C, 23.7; H 3.7; N 7.6; S, 16.3.

$[W_3(SbPh_3)Se_4(acac)_3(py)_3]PF_6$ (4-SbPh). In a similar way, greenish-brown crystals of the compound were obtained from $[W_3Se_4(acac)_3(py)_3]PF_6$ (0.5 g, 0.34 mmol) in CH_3CN and $SbPh_3$ (0.14 g, 0.40 mmol). Yield 30% (0.18 g). Anal. Calcd for $W_3SbC_{48}H_{51}O_6N_3Se_4$: C, 32.85; N, 2.39; H, 2.93. Found: C, 31.96; N, 2.42; H, 2.99. IR (cm^{-1}, KBr): 3446(m), 3335(m), 3208(w), 3151(w), 3122(w), 3045(w), 2922(w), 2855(w), 1648(m), 1608(m), 1573(s), 1531(s), 1491(m), 1447(s), 1430(s), 1370(s), 1283(m), 1189(w), 1157(w), 1069(s), 1026(s), 936(w), 840(s), 737(s), 696(s), 671(s), 558(s), 456(m), 434(s).

$[W_3(SbI_3)Se_4(acac)_3(py)_3]I_3$ (4-SbI). In a similar way, brown crystals of the compound were obtained from $[W_3Se_4(acac)_3(py)_3]PF_6$ (0.5 g, 0.34mmol) and SbI_3 (0.5 g, 1.00 mmol) in acetonitrile. Yield 35% (0.26 g). IR (cm^{-1}, KBr): 3431(m), 3087(w), 2910(w), 2288(w), 1730(w), 1635(w), 1604(w), 1560(vs), 1529(vs), 1440(w), 1422(m), 1358(s), 1283(s), 1221(w), 1189(w), 1068(w), 1027(s), 939(m), 841(vs), 745(m), 687(w), 672(s), 558(s), 440(s).

X-ray Crystallography. Diffraction data were collected at room temperature using a Bruker-Nonius Kappa CCD diffractometer with graphite monochromated Mo Kα radiation ($\lambda = 0.71073$ Å). Frames were collected with the *COLLECT* program,[8] indexed and processed using *Denzo SMN*, and the files were scaled together using the *HKL2000* program.[9] The absorption correction was applied using a semiempirical method based on multiple scanned reflections on *PLATON* program.[10] The structure solution was obtained by direct methods using the *SIR2004* program[11] and refined using the *SHELXL-97* program.[12]

Suitable crystals for X-ray diffraction for **1′-SnCl** were grown by slow evaporation of sample solutions in dichloromethane. The data collection was performed on a Bruker Smart CCD diffractometer using graphite monochromated Mo Kα radiation ($\lambda = 0.71073$ Å). A hemisphere of data was collected based on three ω scans runs (starting $\omega = -28°$) at values $\phi = 0$, 90, and 180° with the detector at $2\theta = 28°$. At each of these runs, frames (606, 435, and 230 respectively) were collected at 0.3° intervals and at 20 s per frame. The diffraction frames were integrated using the *SAINT* package and corrected for absorption with *SADABS*.[13] The positions of the heavy atoms were determined by direct methods and successive difference electron density maps using the *SHELXTL 5.10* software package were done to locate the remaining atoms.[14] Refinement was performed by the full-matrix-least-square method based on F^2. All of the atoms were refined anisotropically, except that the positions of hydrogen atoms were generated geometrically, and were assigned isotropic thermal parameters and allowed to ride on their respective parent C atoms. Tables 1 and 2 list the crystal data, structure refinement details, and the main bond distances. The crystallographic data have been deposited in the Cambridge Crystallographic Data Center under the deposition codes CCDD 656576−656584.

Computational Details. All of the DFT calculations were carried out with the *ADF* program[15] by using triple-ζ and one polarization Slater basis sets to describe the valence electrons of all atoms. Core electrons (e.g., 1s for second period, 1s2s2p for the third period, 1s2s2p3s3p for the fourth period, 1s2s2p3s3p3d4s4p for the fifth period, and 1s2s2p3s3p3d4s4p4d for the sixth period) were treated by a double-ζ basis set using the frozen-core approximation.[15] An auxiliary set of s, p, d, f, and g STOs was used to fit the molecular density and to represent the Coulomb and exchange potentials accurately in each SCF cycle. We used the local spin density approximation, characterized by the electron gas exchange (Xa with $x = 2/3$) together with Vosko−Wild−Nusair parametrization[16] for correlation. Becke's nonlocal correction[17] to the exchange energy and Perdew's nonlocal corrections[18] to the correlation energy were added. Scalar relativistic corrections were included self-consistently by means of the zeroth-order regular approximation [19] using corrected core potentials. The quasirelativistic frozen core shells were generated with the auxiliary program *DIRAC*.[19] The basis set superposition error was estimated using the counterpoise correction.[20]

Results and Discussion

Synthesis and Spectroscopy. The synthesis of the compounds studied in this work is straightforward and is done by mixing the cluster and an EX_3 material and leaving the resulting solution to crystallize. In some cases, partial hydrolysis or oxidation of EX_3 generates new anionic species, like the I_3^- and I_5^- in the reactions with SbI_3, and $[Sb_2Cl_6O]^{2-}$ in the reactions with $SbCl_3$. During the preparation of **2-SnCl**, coordinated pyridine was substituted by acetonitrile.

Analysis of the cuboidal clusters by ESI-MS reveals the presence only of $[Mo_3S_4Cl_3(dmpe)_3]^+$ and $[M_3Q_4(acac)_3(py)_3]^+$ through dissociation of the cuboidal cluster in the ESI chamber. In the case of $(Et_4N)_5[W_3(SbI_3)S_4(NCS)_9]$ (**3-SbI−NCS**), the heaviest peak is of $[W_3S_4(NCS)_6]^{2-}$ ($m/z = 515$), resulting from SbI_3 and NCS^- loss. Significant differences were found in the UV-vis spectra upon changing the polarity of the solvent. To examine in detail the effect of

---

(8) *Collect Program Suite*; Bruker-Nonius: The Netherlands, 1997−2000.

(9) Otwinowski, Z.; Minor, W. Processing of X-ray Diffraction Data Collected in Oscillation Mode. In *Methods in Enzymology*, Macromolecular Crystallography, A; Carter, C. W., Jr., Sweet, R. W., Eds.; Academic Press: New York; Vol. 276, pp 307−326.

(10) Speck, A. L. *Acta Crystallogr.* **1990**, *A46*, C34.

(11) Burla, M. C.; Caliandro, R.; Camalli, M.; Carozzini, B.; Cascarazzo, G. L.; De Caro, L.; Giacovazzo, C.; Polidori, G.; Spagna, R. Sir2004: An Improved Tool for Crystal Structure Determination and Refinement. *J. Appl. Crystallogr.* **2005**, *38*, 381.

(12) Sheldrick, G.M. *SHELXL-97, Program for the Refinement of Crystal Structures*; University of Göttingen: Göttingen, Germany, 1997.

(13) *Bruker SADABS, Area Detector Absorption and Other Corrections*, version 2.03; Delft: The Netherlands, 2002.

(14) *SHELXTL*, version 5.10; Bruker AXS Inc.: Madison, Wisconsin, U.S.A., 1998.

(15) Velde, G. T.; Bickelhaupt, F. M.; Baerends, E. J.; Guerra, C. F.; Van Gisbergen, S. J. A.; Snijders, J. G.; Ziegler, T. *J. Comput. Chem.* **2001**, *22*, 931−967.

(16) Vosko, S. H.; Wilk, L.; Nusair, M. *Can. J. Phys.* **1980**, *58*, 1200−1211.

(17) (a) Becke A. D.; *J. Chem. Phys.* **1986**, *84*, 4524−4529. (b) Becke, A. D. *Phys. Rev. A* **1988**, *38*, 3098−3100.

(18) (a) Perdew, J. P. *Phys. Rev. B* **1986**, *33*, 8822−8824. (b) Perdew, J. P. *Phys. Rev. B* **1986**, *34*, 7406−7406.

(19) Vanlenthe, E.; Baerends, E. J.; Snijders, J. G. *J. Chem. Phys.* **1993**, *99*, 4597−4610.

(20) Boys, S. F.; Bernardi, F. *Mol. Phys.* **1970**, *10*, 553.

Table 1

	1-AsPh	**1′-SnCl**	**2-SnCl**	**3-SbI**	**3-SbPh**
empirical formula	$C_{54}H_{60}AsF_6Mo_3N_6O_6PS_4$	$C_{18}H_{48}Cl_6Mo_3P_6S_4Sn$	$C_{21}H_{37}Cl_3Mo_3N_3O_8Se_4Sn$	$C_{30}H_{36}I_8N_3O_6S_4SbW_3$	$C_{48}H_{51}F_6N_3O_6PS_4SbW_3$
fw	1525.03	1197.83	1288.24	2351.36	1712.43
cryst syst	triclinic	hexagonal	monoclinic	monoclinic	triclinic
space group	$P\bar{1}$	$R3c$	$P2_1/c$	$P2_1/m$	$P\bar{1}$
			Unit Cell Dimensions		
a (Å)	12.5376(3)	17.117(4)	$a = 10.8620(10)$	10.974(2)	12.7664(3)
b (Å)	16.0973(3)	17.117(4)	$b = 19.2860(10)$	19.440(4)	16.4865(5)
c (Å)	16.7835(5)	24.124(7)	$c = 22.2305(10)$	12.671(3)	16.9376(4)
α (deg)	97.5270(10)				98.1260(10)
β (deg)	106.9250(10)		119.076(3)	95.60(3)	107.3310(10)
γ (deg)	99.4630(10)				99.8570(10)
V (Å^3)	3138.52(13)	6121(3)	4070.1(5)	2690.2(9)	3281.96(15)
Z	2	6	4	2	2
ρ_{calcd} (g cm^{-3})	1.614	2.353	2.102	2.903	1.733
$F(000)$	1532	3528	2444	2092	1628
2θ (deg)	2.58−55.00	2.18−30.00	1.49−28.65	2.57−25.00	2.56−55.00
reflns/unique	35 611/14 218 [R(int) = 0.0358]	15 950/3947 [R(int) = 0.0671]	44 392/9803 [R(int) = 0.0785]	40 466/4833 [R(int) = 0.0471]	31 955/14 873 [R(int) = 0.0276]
params/restraints	695/0	112/1	398/0	266/0	659/0
GOF	1.019	0.924	1.180	1.254	1.098
R1 ($I > 2\sigma(I)$)	0.0448	0.0360	0.0535	0.0465	0.0370
wR2 (all data)	0.1152	0.0693	0.1456	0.1287	0.1289
	3-PbI	**3-SbCl′**	**3-SnCl**[a]	**4-SbPh**	**4-SbI**
empirical formula	$C_{33.40}H_{41..10}I_3\ N_{4.70}O_6PbS_4W_3$	$C_{40}H_{51}Cl_9N_5O_8S_4Sb_3W_3$	$C_{30}H_{36}Cl_3N_3O_6S_4SnW_3$	$C_{45}H_{51}F_6N_6O_6PSbSe_4W_3$	$C_{26}H_{35}I_6N_4O_6SbSe_4W_3$
fw	1872.09	2093.95	1439.45	1906.03	2250.12
cryst syst	monoclinic	triclinic	monoclinic	triclinic	monoclinic
space group	$C2/m$	$P\bar{1}$	$P2_1/m$	$P\bar{1}$	$C2/m$
			Unit Cell Dimensions		
a (Å)	24.597(5)	12.0411(7)	11.072(2)	12.901(3)	22.9402(6)
b (Å)	13.461(3)	18.0061(14)	18.862(4)	16.661(3)	13.4517(3)
c (Å)	15.187(3)	19.4070(15)	11.938(2)	17.125(3)	19.5758(5)
α (deg)	90	114.99	90	98.36(3)	90
β (deg)	99.47(3)	93.080(3)	96.33(3)	107.44(3)	123.4150(10)
γ (deg)	90	108.040(4)	90	100.79(3)	90
V (Å^3)	4959.9(17)	3542.0(4)	2477.9(9)	3368.9(12)	5042.3(2)
Z	4	2	2	2	4
ρ_{calcd} (g cm^{-3})	2.507	1.963	1.929	1.879	2.964
$F(000)$	3398	1964	1344	1778	3976
2θ (deg)	5.44−50.00	4.60−57.24		5.50−50.00	2.50−55.00
reflns/unique	43688/4572 [R(int) = 0.0706]	92850/17354 [R(int) = 0.1226]		48762/11816 [R(int) = 0.0966]	20450/5983 [R(int) = 0.0306]
params/restraints	281/0	658/0		650/0	257/0
GOF	1.274	1.105		1.188	1.063
R1 ($I > 2\sigma(I)$)	0.0611	0.0569		0.0644	0.0377
wR2 (all data)	0.1654	0.1723		0.1776	0.0934

[a] The structure refinement was not completed due to the low quality of the crystal.

the solvent on the spectroscopic features, UV-vis spectra were recorded in CH_2Cl_2/CH_3CN mixtures at different solvent ratios. On dilution with CH_3CN, a gradual yellow-to-green color change takes place accompanied by a bathochromic shift of the band centered at 331 nm and the disappearance of the band centered on 469 nm. The UV-vis spectrum of **1′-SnCl** in neat CH_3CN was identical to that of its trinuclear precursor $[Mo_3S_4Cl_3(dmpe)_3]^+$, thus suggesting easy dissociation in CH_3CN solutions. This experimental evidence can be interpreted in terms of ion pairing on going from CH_3CN to CH_2Cl_2. In CH_2Cl_2 solutions, the spectral changes may be due to charge-transfer between $[Mo_3S_4Cl_3(dmpe)_3]^+$ and $SnCl_3^-$, possibly mediated by weak Sn···S contacts as found in the solid:

$$\{[Mo_3S_4Cl_3(dmpe)_3]SnCl_3\} = [Mo_3S_4Cl_3(dmpe)_3]^+ + SnCl_3^-$$

On the contrary, the solutions of the complexes based on $[M_3Q_4(acac)_3(py)_3]^+$ both in CH_2Cl_2 and CH_3CN do not indicate any dissotiation, except for **1-AsPh**, which is again in a good agreement with structural data, as discussed below.

Structure Features. EPh_3 Derivatives. Compound **1-AsPh** can be regarded as a weakly bound associate of $[Mo_3S_4(acac)_3(py)_3]^+$ and $AsPh_3$ (Figure 1). The As atom forms two short and one long contact with the three μ_2-S atoms of the cluster. The As−S distances (Table 2) are much longer than expected for a covalent single bond. However, some shortening of Mo−Mo bonds (by ca. 0.01−0.03 Å) as compared with the parent $[Mo_3S_4(acac)_3(py)_3]^{+5}$ indicates that the cluster does *feel* the weak coordination of $AsPh_3$. The coordination polyhedron around As must be regarded as a very irregular [3+3] octahedron with C−As−C angles ranging from 98.6 to 100.3° and trans C−As−S angles from 127.7 to 160.3°. The effect of coordination on the $AsPh_3$ molecule is reflected in a slight lengthening of As−C bonds (from 1.954(av) to 1.962(av) Å), and equally slight changes

Table 2. Main Bond Distances in the Cuboidal and Parent Triangular Clusters

cluster	M−M	M−Q	M′−Q	M′−X	f_{cov} M′−Q
$[Mo_3(AsPh_3)S_4(acac)_3(py)_3]PF_6\langle 3MeCN$ **(1-AsPh)**	2.729(1)	2.289(2)−2.307(1)	3.087(2)	1.955(5)	0.46[a]
	2.746(2)		3.381(1)	1.966(4)	
	2.735(1)		3.133(3)	1.966(6)	
$[Mo_3(SnCl_3)S_4Cl_3(dmpe)_3]$ **(1′-SnCl)**	2.7257(9)	2.284(2)−2.328(2)	3.241(2)	2.466(2)	0.52
$[Mo_3(SnCl_3)S_4(NCS)_9]^{6-}$	2.730(2)	2.340(3)	2.616(3)	2.446(4)	0.93
			2.664(3)	2.467(4)	
			2.666(3)	2.474(3)	
$[Mo_3(SnCl_3)S_4(dtp)_3(py)_3]$	2.713(2)	2.319(2)−2.344(2)	2.682(3)	2.410(4)	0.86
	2.716(2)		2.733(3)	2.406(4)	
	2.725(2)		2.716(3)	2.409(4)	
$[Mo_3(PbI_3)S_4(dtp)_3(py)_3]$	2.751(2)	2.289(2)−2.338(2)	3.099(3)	2.944(4)	0.65
	2.747(1)		3.124(3)	2.914(4)	
	2.744(2)		3.128(3)	2.938(4)	
$[Mo_3S_4(acac)_3(py)_3]PF_6$	2.7625(9)	2.291(1)			
$[Mo_3(SnCl_3)Se_4(acac)_3(CH_3CN)_3]\cdot 2H_2O$ **(2-SnCl)**	2.758	2.446−2.461	2.844	2.429	0.88
	2.757		2.804	2.457	
			2.822	2.464	
$[Mo_3(SnCl_3)Se_4(NCS)_9]^{6-}$	2.805(1)	2.445(2)−2.466(2)	2.782(1)	2.442(3)	0.91
	2.779(1)		2.734(1)	2.468(2)	
	2.777(1)		2.805(1)	2.471(3)	
$[Mo_3(SnCl_3)Se_4Cl_2(H_2O)_7]^{+}$	2.760(1)	2.436(2)−2.451(2)	2.804(2)	2.443(3)	0.89
	2.760(1)		2.804(2)	2.443(3)	
	2.778(1)		2.824(2)	2.449(3)	
$[W_3(PbI_3)S_4(acac)_3(py)_3]\cdot 1.7CH_3CN$ (**3-PbI**)	2.737(1)	2.313−2.317	3.22(3)	2.90(3)	0.59[a]
	2.745(3)		3.22(3)	2.98(2)	
	2.745(3)		3.49(4)	2.98(2)	
$[W_3(PbI_3)S_4(dtp)_3(py)_3]$	2.739(2)	2.288(3)−2.346(3)	3.159(3)	2.947(4)	0.63
	2.741(2)		3.182(3)	2.968(5)	
	2.749(3)		3.116(3)	2.925(4)	
$[W_3(SbCl_3)S_4(acac)_3(py)_3]^{+}$ **(3-SbCl′)**	2.745(5)	2.326(4)−2.330(4)	2.845(6)	2.393(7)	0.73
	2.751(1)		2.873(4)	2.398(4)	
	2.746(7)		2.880(4)	2.401(4)	
$[W_3(SbCl_3)S_4Cl_3(H_2O)_6]^{+}$	2.710	2.300−2.349	2.845	2.409	0.75
$[W_3(SnCl_3)S_4(acac)_3(py)_3]$ (**3-SnCl**)	2.76(1)	2.32(2)−2.39(2)	2.78(3)	2.466	0.78
			2.88(3)	2.532	
			2.88(3)	2.532	
$[W_3(SnCl_3)S_4(NCS)_9]^{6-}$	2.730(1)	2.327(4)−2.345(4)	2.713(4)	2.492(7)	0.84
	2.743(1)		2.744(4)−2.768(5)	2.500(5)	
	2.746(1)			2.512(5)	
$[W_3(SnCl_3)S_4(dtp)_3(py)_3]$	2.706(1)	2.316(2)−2.355(2)	2.726(3)	2.435(5)	0.82
	2.709(1)		2.809(3)	2.422(5)	
	2.720(1)		2.796(3)	2.432(5)	
$[W_3(SbI_3)S_4(acac)_3(py)_3]I_5$ **(3-SbI)**	2.74(1)	2.32(2)−2.33(2)	2.89(3)	2.77(2)	0.80
	2.75(1)		2.89(3)	2.77(2)	
	2.75(1)		2.90(3)	2.77(4)	
$[W_3(SbI_3)S_4(OAc)(dtp)_3(py)]$	2.680(1)	2.311(2)−2.356(3)	2.780(4)	2.781(5)	0.78
	2.741(1)		2.867(4)	2.764(5)	
	2.735(1)		2.892(4)	2.810(4)	
$[W_3(SbPh_3)S_4(acac)_3(py)_3]PF_6$ **(3-SbPh)**	2.737(2)	2.308(2)−2.321(2)	3.167	2.141(10)	0.56[a]
	2.724(2)		3.116	2.173(7)	
	2.719(1)		3.338	2.162(9)	
$[W_3S_4(acac)_3(py)_3]PF_6$	2.7485(5)	2.308(1)			
$[W_3(SbPh_3)Se_4(acac)_3(py)_3]PF_6$ (**4-SbPh**)	2.76(3)	2.44(5)−2.45(3)	3.12(4)	2.14(3)	0.64[a]
	2.78(5)		3.15(9)	2.16(6)	
	2.76(3)		3.32(2)	2.16(3)	
$[W_3(SbI_3)Se_4(acac)_3(py)_3]I_3$ **(4-SbI**)	2.768(0)	2.449(1)−2.460(2)	2.918(1)	3.15(9)	0.78
	2.781(2)		2.931(3)	3.32(2)	
	2.781(2)		2.918(1)	3.12(4)	
$[W_3(SnCl_3)Se_4(NCS)_9]^{6-}$	2.768(1)	2.46(1)−2.47(1)	2.800(4)	2.480(5)	0.86
	2.778(1)		2.883(4)	2.510(6)	
	2.786(1)		2.857(4)	2.514(4)	
$[W_3Se_4(acac)_3(py)_3]PF_6$	2.8069(8)	2.4290(9)			

[a] A middle value from the two shorter distances was used to calculate f_{cov}.

of one of the C−As−C angles (decrease by up to 2°). Similar structural features are encountered in **3-SbPh**, except that here both Sb−C bond lengths and the C−Sb−C angles increase upon coordination (by 0.01(av) Å and 1.5(av)°). In the analogue, **4-SbPh**, the average lengthening of the Sb−C bonds is also about 0.01 Å and the C−Sb−C bond angles are by 2° larger than those in the free $SbPh_3$ molecule.[21]

---

(21) (a) Sobolev, A. N.; Belsky, V. K.; Chernikova, N. Yu.; Akhmadulina, F. Yu. *J. Organomet. Chem.* **1983**, *244*, 129 ($AsPh_3$). (b) Adams, E. A.; Kolis, J. W.; Pennington, W. T. *Acta Crystallogr., Sect. C* **1990**, *46*, 917 ($SbPh_3$).

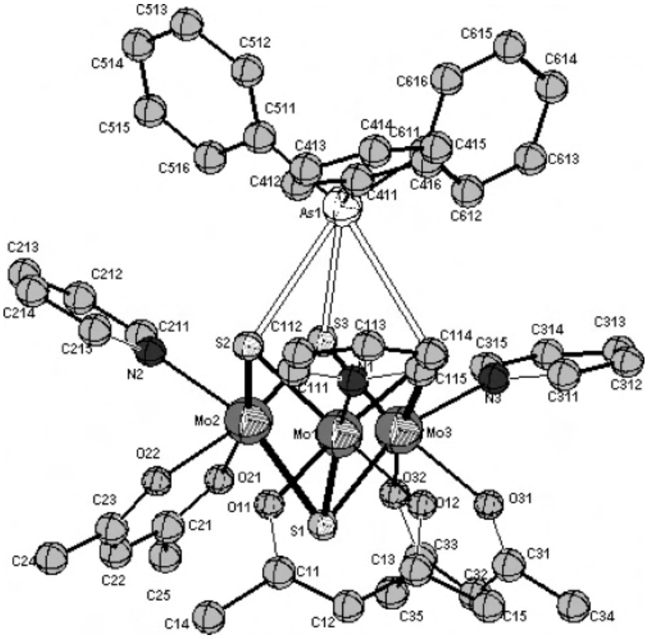

Figure 1. ORTEP representation of **1-AsPh** showing an atom numbering scheme. The hydrogen atoms are omitted for clarity.

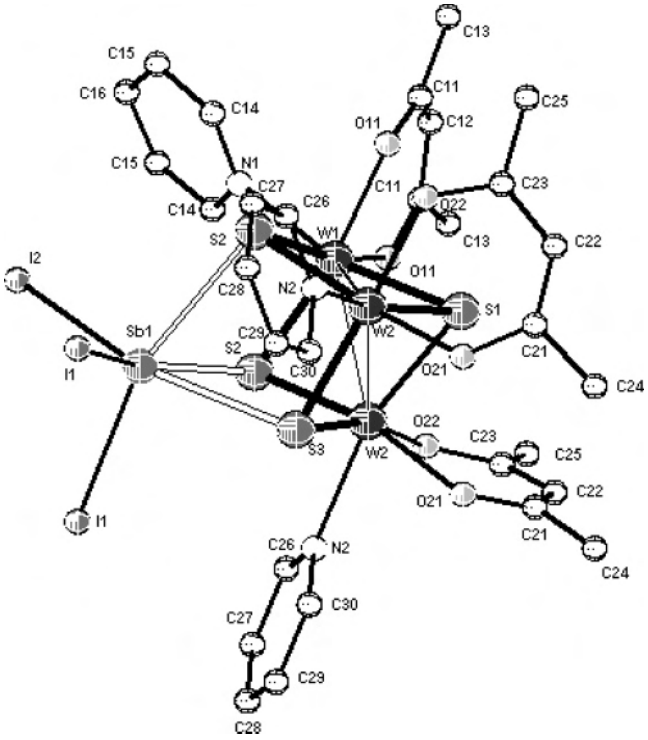

Figure 2. ORTEP representation of **3-SbI** showing an atom numbering scheme. The hydrogen atoms are omitted for clarity.

SbX_3 Derivatives. In all of the cases, and unlike the situation with the $SbPh_3$ complexes, the SbX_3 units are coordinated symmetrically to the three μ_2-Q atoms of the parent trinulclear cluster, and the coordination around Sb atoms is more regularly octahedral. Scrutiny of Sb−S bond lengths in the W_3S_4 derivatives (**3-SbCl′** and **3-SbI,** Figure 2) leaves the impression of a somewhat stronger coordination of $SbCl_3$. The effects, however, are small and may just reflect the different packing forces of different counter-ions ($Sb_2OCl_6^{2-}$ and I_5^-, respectively). Comparison of the geometrical parameters of the coordinated SbX_3 units with the geometry of free SbX_3 molecules (in gas phase) shows significant bond lengthening and valence angle decrease upon coordination: from 2.333 Å (97.2°) in free $SbCl_3$ (gas phase) to 2.39−2.40 Å (93.7−94.6°) in **3-SbCl′**, and from 2.719 Å (99°) in free SbI_3 to 2.77−2.78 Å (96.8−99.9°) in **3-SbI**, and to 2.80−2.81 Å (96.9 − 97.7°) in **4-SbI.** In solid $SbCl_3$ and SbI_3, the Sb−X bonds are also longer, 2.359(av) Å in $SbCl_3$ and 2.765 Å in SbI_3.[22] What is more important, in both solids there are secondary Sb···X bonding interactions, which in the case of SbI_3 complete the coordination around Sb to distorted octahedral. This secondary bonding is described as arising from electron density donation onto Sb−X σ* orbitals.[23]

The coordination of EX_3 to the three sulfur atoms of the M_3S_4 core can be formally compared to the formation of the complexes EX_3 with 1,4,7-trithiacyclononane, [9]-ane−S3. In the resulting octahedral complexes, the E−S distances are 2.72−2.86 Å (with $AsCl_3$), 2.84−2.90 Å (with SbI_3), and 3.15−3.40 Å (with $SbCl_3$).[24] This data show that the M_3S_4 clusters and [9]-ane-S3 are comparable in strength as ligands for SbX_3. Curiously, in adduct $SbI_3 \cdot 3S_8$, the intermolecular contacts formed only through S···I contacts, without any Sb participation.[25]

Sn and Pb Derivatives. These are neutral molecules because the charge of the parent cluster cation is neutralized by the uninegative $SnCl_3^-$ and PbI_3^- (Figure 2). This is probably the reason for the virtual absence of M−M bond shortening upon the formation of the corresponding clusters, **2-SnCl**, **3-SnCl**, and **3-PbI**, because the electrostatic component of the packing forces is different and these forces may account for as much as a 0.05 Å change in the M−M bond lengths. The Sn and Pb atoms are in a distorted octahedral environment and are coordinated less symmetrically than the antimony halides (trans S−Sn−Cl angles 163.5−163.9°), and have the shortest Sn−Cl bonds in the trans position to the longest Sn−S bond, and vice versa. Similar structural features are observed in the lead cluster **3-PbI** (S−Pb−I 161.8−154.9°; a longer Pb−I bond (2.981 Å) in the trans position to the shortest Pb−S contact (3.217 Å), and a shorter Pb−I bond (2.898 Å) in the trans position to the longer Pb−S contact (3.485 Å). In free $SnCl_3^-$, the Sn−Cl distances are 2.46−2.56 Å long, whereas in the octahedral $SnCl_6^{2-}$ they are about 2.42 Å.[26] No salts of discrete PbI_3^- ion exist. The most significant feature of **1′-**

---

(22) (a) Lipka, A. *Acta Crystallogr., Sect. B* **1979**, *3020*, 35. (b) Pohl, S.; Saak, W. *Z. Kristallogr.* **1984**, *169*, 177.

(23) (a) Fisher, G. A.; Norman, N. *Adv. Inorg. Chem.* **1994**, *41*, 233. (b) Alcock, N. W. *Bonding and Structure: Structural Principles in Inorganic and Organic Chemistry*; Ellis Horwood: Chichester, U.K., 1990.

(24) (a) Hill, N. J.; Lewason, W.; Reid, G. *Inorg. Chem.* **2002**, *41*, 2070. (b) Pohl, S.; Haase, D.; Peters, M. *Z. Anorg. Allg. Chem.* **1993**, *619*, 727. (c) Willey, G. R.; Lakin, M. T.; Ravindran, M.; Alcock, N. W. *Chem. Commun.* **1991**, 271.

(25) Bjorvatten, T.; Hassel, O.; Lindheim, A. *Acta Chem. Scand.* **1963**, *17*, 689.

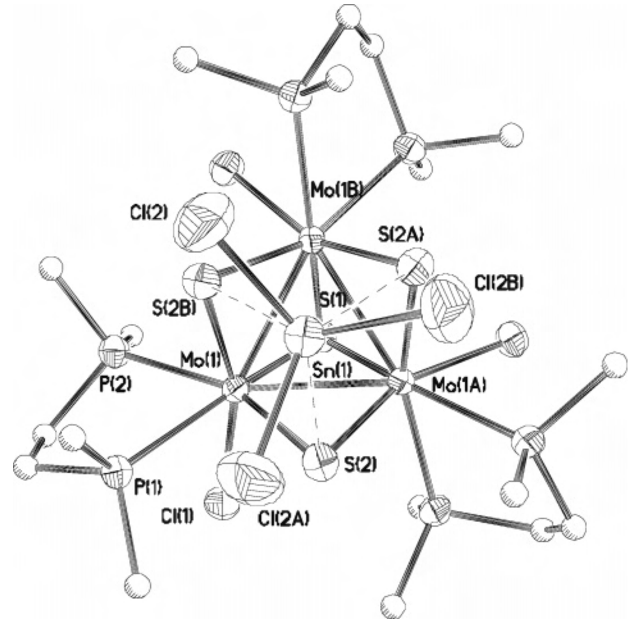

Figure 3. ORTEP representation of the **1′-SnCl** compound with an atom numbering scheme.

Table 3. ADF/BP86/TZP Optimized Geometrical Parameters (Angstroms)

	$[W_3(SbI_3)S_4(acac)_3(py)_3]^+$	$[W_3(SbPh_3)S_4(acac)_3(py)_3]^+$	$[W_3(SbI_3)Se_4(acac)_3(py)_3]^+$	$[W_3(SbPh_3)Se_4(acac)_3(py)_3]^+$
Sb−Q2	3.150	3.291	3.128	3.304
Sb−Q3	3.172	3.304	3.131	3.340
Sb−Q4	3.146	3.457	3.138	3.508
W−W	2.788	2.774	2.842	2.820
W−Q1	2.412	2.389	2.524	2.523
W−Q2	2.349	2.345	2.479	2.477

SnCl is the anomalously elongated Sn−S distance (3.240(2) Å). This loose attachment of the $SnCl_3$ fragment on the trinuclear core is due to the presence of the bulky diphosphanes, which prevent the approximation of the $SnCl_3$ fragment. This orientation of the $SnCl_3$ group contrasts with all of the other $M_3(EX_3)Q_4$ cluster cores where the dihedral angles M−Q−E−X are close to zero, that is, the X atoms eclipse the M atoms. As seen in Figure 3, this disposition is not favored in **1′-SnCl**, where the $SnCl_3$ unit is rotated away by 38°. Therefore, the formation of heterometallic clusters based on $[Mo_3S_4Cl_3(dmpe)_3]^+$ with the heterometal in an octahedral environment seems to be hindered by the steric factors. Conversely, incorporation of other heterometals such as Co, Ni, and Cu has been easily achieved where the heterometal appears in a tetrahedral environment.[27] In other compounds with weaker E···Q contacts (the EPh_3 adducts or **3-PbI**), packing forces also force the EX_3 unit out of the eclipsed conformation by some 10−19°.

From the analysis of the E···Q distances (Table 2), it is clearly seen that the interaction between the EX_3 unit and the triangular cluster is not very strong. To analyze such contacts, a semiempirical parameter, termed the covalency factor (f_{cov}) was found to be useful. To the value $f_{cov} = 0$ corresponds no bonding, to $f_{cov} = 1$ − normal bonding. It is calculated as $f_{cov} = [R_{vdW}(Q) + R_{vdW}(X) - d(Q_{ax}-X)][R_{vdW}(Q) + R_{vdW}(X) - R_{cov}(Q) - R_{cov}(X)]^{-1}$, where R_{vdW} and R_{cov} are the van der Waals radii and covalent radii of the corresponding atoms.[28] In our cases, the strongest bonding is achieved for the $SnCl_3^-$ (f_{cov} 0.8−0.9). M_3Q_4 binds the EX_3 units less stronger than the Fe_3Se_4 core in $[Cp^*{}_3Fe_3Se_4(SnCl_3)]$ (Sn−Se 2.67 Å $f_{cov} = 0.98$).[29] The affinity of the cluster core for $SnCl_3^-$ decreases in the row ($Fe_3Se_4^{4+}$) > $Mo_3S_4^{4+}$ > $Mo_3Se_4^{4+}$ > $W_3Se_4^{4+}$ > $W_3S_4^{4+}$, in perfect agreement with the observed reactivity patterns of the $[M_3(SnCl_3)Q_4(H_2O)_9]^{3+}$ clusters and the redox potential of the M_3Q_4 core.[5,30] The model of electron transfer from Sn(II) to the M_3Q_4 core as the driving force for the formation and stability of the cuboidal clusters seems to hold. The unusually weak interaction in **1′-SnCl** can be explained both by sterical reasons and by the influence of the strongly basic dmpe ligand, which reduces the electronegativity of the cluster core. The much weaker interaction of the isoelectronic PbI_3^- (f_{cov} of about 0.6) is clearly due to the increased stability of the Pb(II) state. For group 15, the situation is more complicated. The EPh_3 molecules are capable only of formation of weak adducts (f_{cov} of about 0.6). The halides bind stronger, with a f_{cov} around 0.7−0.8, and in the order SbI_3 > $SbCl_3$; W_3Se_4 > W_3S_4. The interaction of $SbCl_3$ with the $Ir_3S_4^{3+}$ core in $[Cp^*{}_3Ir_3S_4(SbCl_3)]$ is much stronger (Sb−S, 2.55 Å; f_{cov} =

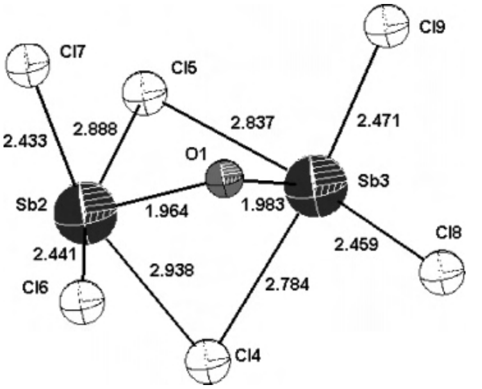

Figure 4. $[Sb_2OCl_6]^{2-}$ anion in **3-SbCl′**.

Table 4. Contributions to the Total Complex Interaction Energies (kcal/mol) According to the Energy Decomposition Analysis Using BP86/TZP Calculations

	$[W_3(SbI_3)S_4(acac)_3(py)_3]^+$	$[W_3(SbPh_3)S_4(acac)_3(py)_3]^+$	$[W_3(SbI_3)Se_4(acac)_3(py)_3]^+$	$[W_3(SbPh_3)Se_4(acac)_3(py)_3]^+$
ΔE_{es}	−30.85	−23.64	−42.68	−29.22
ΔE_{Pauli}	+53.78	+42.82	+74.5	+49.96
ΔE_{oi}	−33.73	−23.35	−46.65	−27.31
ΔE_{int}	−10.8	−4.17	−14.83	−6.57
ΔE	−9.21	−2.70	−12.73	−3.85
BSSE	−2.36	−0.99	−2.74	−1.07

---

[26] See, for example (a) Mercier, N.; Seyeux, A.; Morel, C.; Riou, A. *Acta Crystallogr., Sect. C* **2002**, *58*, m127. (b) Müller, U.; Mironga, N.; Schumacher, C.; Dehnicke, K. *Z. Naturforsch.* **1982**, *37b*, 1122. ($SnCl_3^-$) (c) Knop, O.; Cameron, T.S.; James, M.A.; Falk, M. *Can. J. Chem.* **1983**, *61*, 1620. ($SnCl_6^{2-}$).

[27] Llusar, R.; Uriel, S. *Eur. J. Inorg. Chem.* **2003**, 1271.

[28] Batsanov, S. S. *Russ. J. Inorg. Chem.* **1991**, *36*, 1694.

[29] Zimmermann, C.; Anson, C. E.; Eckermann, A. L.; Wunder, M.; Fisher, O.; Keilhauer, I.; Heerling, E.; Pikrwa, B.; Hampe, O.; Weigend, F.; Dehnen, S. *Inorg. Chem.* **2004**, *43*, 4595.

[30] Fedin, V. P.; Dybtsev, D. N. *Zh. Neorg. Khim.* **1999**, *44*, 743.

Table 5. Mulliken (M), Hirshfeld (H) and Voronoi Deformation Density (VDD) Atomic Charges of the W_3S_4 and W_3Se_4 Complexes

	$[W_3(SbI_3)S_4(acac)_3(py)_3]^+$			$[W_3(SbPh_3)S_4(acac)_3(py)_3]^+$			$[W_3(SbI_3)Se_4(acac)_3(py)_3]^+$			$[W_3(SbPh_3)Se_4(acac)_3(py)_3]^+$		
atom	M	H	VDD	M	H	VDD	M	H	VDD	M	H	VDD
W1	1.02	0.29	0.25	1.00	0.28	0.24	1.16	0.25	0.21	1.16	0.23	0.19
W2	1.02	0.29	0.25	0.98	0.27	0.24	1.17	0.25	0.21	1.15	0.23	0.19
W3	1.02	0.29	0.25	0.98	0.27	0.23	1.17	0.25	0.21	1.14	0.23	0.19
Q (μ_3)	−0.22	−0.08	−0.15	−0.22	−0.08	−0.15	−0.34	−0.02	−0.10	−0.36	−0.02	−0.10
Q (μ_2)	−0.30	−0.11	−0.20	−0.30	−0.11	−0.21	−0.44	−0.06	−0.15	−0.46	−0.08	−0.19
Q (μ_2)	−0.31	−0.11	−0.20	−0.29	−0.13	−0.23	−0.45	−0.06	−0.16	−0.48	−0.09	−0.20
Q (μ_2)	−0.30	−0.11	−0.20	−0.31	−0.12	−0.22	−0.43	−0.06	−0.15	−0.45	−0.07	−0.17
Sb	0.21	0.32	0.34	1.29	0.35	0.25	0.24	0.30	0.33	1.39	0.35	0.25
X = I,Ph	−0.10	−0.15	−0.17	−0.48	−0.04	−0.12	−0.09	−0.16	−0.18	−0.51	−0.08	−0.11
X = I,Ph	−0.10	−0.14	−0.17	−0.51	−0.04	−0.11	−0.09	−0.16	−0.18	−0.48	−0.08	−0.11
X = I,Ph	−0.10	−0.15	−0.17	−0.50	−0.04	−0.12	−0.09	−0.15	−0.18	−0.50	−0.08	−0.12

0.93).[31] To understand this weaker interaction, we have performed quantum-chemical calculations on the $[W_3Q_4(acac)_3(py)_3]^+/SbX_3$ (Q = S, Se; X = I, Ph) systems.

Anionic Part. The structure of **3-SbCl′** contains binuclear oxochloroantimonate(III) $[Sb_2(\mu\text{-}O)(\mu\text{-}Cl)_2Cl_4]^{2-}$ (Figure 4), which arises from partial hydrolysis of $SbCl_3$. Its main geometric parameters are very close to those observed in the salt $(pyH)_2[Sb_2OCl_6]$.[33] The I_3^- and I_5^- anions in **4-SbI** and **3-SbI**, respectively, arise from partial hydrolysis and air oxidation of SbI_3, which was taken in a considerable excess. The triodide in **4-SbI** is in usual symmetric conformation (I−I, 2.896 and 2.916 Å; ∠I−I−I, 178.8°). The V-shaped pentaiodide in **3-SbI** (∠I−I−I (central) 111° has two short (2.822 Å, periferic) and two long (3.054 Å, central) I−I bonds.

Theoretical Calculations. The interaction between $[W_3Q_4(acac)_3(py)_3]^+$ (Q = S, Se) and SbX_3 (X = I, Ph) is of the closed-shell type, and the formation of the cubane is not allowed. However, the orientation of SbX_3 toward the three chalcogen atoms of the trinuclear cluster suggests the existence of stabilizing electrostatic (polarization) and orbital interactions. Further insight into the energy of the interaction can be gained using a quantitative energy decomposition scheme. Although the partition of intermolecular interactions is not unique, several strategies have been proposed to assess the electrostatic or covalent character of the interaction. Because of the size of this system, we will be limited to the energy decomposition analysis of Baerends et al.,[32] which allows us to distinguish between electrostatic, exchange (Pauli) repulsion, and orbital interaction. Energy decomposition analysis of the binding energies has been performed for all of the complexes. The method has been described in detail before and is only briefly described here. The formation of bonding between the two fragments (the triangular cluster (1) and the EX_3 molecule (2)) is divided into three physically plausible steps. In the first step, the fragment electronic densities (in the frozen geometry of the adduct) are superimposed, which yields the quasiclassical electrostatic interaction energy ΔE_{es}. Renormalization and orthogonalization of the product of one fragment wave functions yield a repulsive energy term that is usually called Pauli (exchange) repulsion (ΔE_{Pauli}). In the final step, the molecular orbitals are allowed to relax to their final form, which yields the (stabilizing) polarization, orbital, dispersion, and charge-transfer interaction energy ΔE_{oi}. The interaction energy is defined as

$$\Delta E_{int} = \Delta E_{es} + \Delta E_{Pauli} + \Delta E_{oi} \qquad (1)$$

and differs from the true interaction energy (ΔE_{true}) by the energy necessary to bring the optimum fragment geometries into the form they have in the adduct (ΔE_{prep}):

$$\Delta E_{total} = \Delta E_{prep} + \Delta E_{int} \qquad (2)$$

All of the energy increments are expressed as the difference:

$$\Delta E = \Delta E(1\cdots 2) - \Delta E(1) - \Delta E(2) \qquad (3)$$

Selected BP86/TZP optimized geometrical parameters are listed in Table 3 and show good agreement with those obtained from X-ray crystallography. The components of the interaction energy explained above (ΔE_{es}, ΔE_{Pauli}, ΔE_{oi}), the $\Delta E_{int,}$ the ΔE_{true}, and their BSSE are summarized in Table 4. It should be noted that the BSSE values are small but still represent a considerable part of the interaction energy of some complexes. However, because the size of the system used, larger basis sets are not affordable. The values of ΔE_{prep} are similar for all of the complexes, and for the sake of clarity we will discuss ΔE_{int} rather than ΔE_{true}. The values of ΔE_{int} (from −4.17 to −14.83 kcal/mol) are of the order of medium-to-weak hydrogen bonding. The strongest complex (of the four) is formed between the W_3Se_4 core and SbI_3.

The replacement of iodine by phenyl in EX_3 leads to a decrease in the interaction energy. Table 4 shows that the weakening of the adduct is due to the decreasing electrostatic interactions, whereas Pauli and orbital interaction components partially cancel each other. The electrostatic interaction strengthens the bonding, whereas the sum of Pauli and orbital interactions destabilizes it. The orbital interaction is rather large (23 to 46 kcal/mol) considering the relatively long distance between the interacting units. The assignment of the orbital interaction to the stabilization of a specific molecular orbital is not straightforward. Besides the interaction between the lone pair of Sb pointing toward the three μ_2-S atoms, there are other interactions between the MO of both partners due to the presence of very diffuse valence orbitals.

---

(31) Shinozaki, A.; Seino, H.; Hidai, M.; Mizobe, Y. *Organometallics* **2003**, *22*, 4636.

(32) Bickelhaupt, F. M.; Baerends, E. J. *Rev. Comput. Chem.* **2000**, *15*, 1.

(33) Hall, M.; Sowerby, D. B. *J. Chem. Soc., Chem. Comm.* **1979**, 1134.

Atomic charges calculated using Mulliken, Hirshfeld, and Voronoi deformation density are listed in Table 5. A small transference of electronic density charge (around 0.10 e) can be observed from the W_3Q_4 core to the SbX_3 moiety. The replacement of iodine atoms by Ph groups reduces the positive charge at the Sb atoms (from 0.34 to 0.25), lowering the electrostatic interactions with the negatively charged $Q(\mu_2)$ atoms. Similarly, replacement of $S(\mu_2)$ by $Se(\mu_2)$ atoms reduces the negative charge slightly from −0.20 to −0.15, also decreasing the electrostatic interactions.

In conclusion, the interactions between the M_3Q_4 cluster core and post-transition cations with a lone pare range from strongly covalent to much weaker and predominantly electrostatic, of the order of hydrogen bonding. There is a good correlation between the energy of the interaction as calculated by quantum chemistry and such a simple empirical parameter as covalency factor, which is calculated from the difference in the sum of the van der Waals radii and observed bond lengths. Though the $Mo_3S_4^{4+}$ core (on the part of the cluster unit) and Sn(II) (form all the heterometals studied) usually give the strongest complexes, the situation is also influenced by the spectator ligands in the cluster and even by the solvent. The calculations show that in addition to the charge-transfer model (from M′ to Mo/W), which requires the s^2p^0 configuration of heterometal and explains the decrease in stability in the order Sn > Pb > Sb > As, just as the ionization potential increases,[34] the electrostatic interaction between the heterometal and chalcogen is also important − electronegative substituents at M′ lead to more stable complexes (halides vs phenylic in our case). Both trends can work synergetically, as was suggested in **3b**: the more charge transferred from M′ to Mo/W, the stronger the electrostatic interaction M′−Q becomes.

Acknowledgment. V.P. is thankful for support from the MEC for a JdC research contract and Generalitat Valenciana (GV2007/106 Project). M.N.S. was supported by Grant MD-7072.2006.3.

IC701581U

---

(34) Shriver, D. F.; Atkins, P. W.; Langford, C. H. *Inorganic Chemistry*; Oxford University Press: New York, 1990; p 29.